NANO · MICRO small
www.small-journal.com

Targeted Delivery of Cell Softening Micelles to Schlemm's Canal Endothelial Cells for Treatment of Glaucoma

*Trevor Stack, Michael Vincent, Amir Vahabikashi, Guorong Li, Kristin M. Perkumas, W. Daniel Stamer, Mark Johnson, and Evan Scott**

Increased stiffness of the Schlemm's canal (SC) endothelium in the aqueous humor outflow pathways has been associated with elevated intraocular pressure (IOP) in glaucoma. Novel treatments that relax this endothelium, such as actin depolymerizers and rho kinase inhibitors, are in development. Unfortunately, these treatments have undesirable off-target effects and a lower than desired potency. To address these issues, a targeted PEG-*b*-PPS micelle loaded with actin depolymerizer latrunculin A (tLatA-MC) is developed. Targeting of SC cells is achieved by modifying the micelle surface with a high affinity peptide that binds the VEGFR3/FLT4 receptor, a lymphatic lineage marker found to be highly expressed by SC cells relative to other ocular cells. During in vitro optimization, increasing the peptide surface density increased micellar uptake in SC cells while unexpectedly decreasing uptake by human umbilical vein endothelial cells (HUVEC). The functional efficacy of tLatA-MC, as measured by decreased SC cell stiffness compared to non-targeted micelles (ntLatA-MC) or targeted blank micelles (tBL-MC), is verified using atomic force microscopy. tLatA-MC reduced IOP in an in vivo mouse model by 30–50%. The results validate the use of a cell-softening nanotherapy to selectively modulate stiffness of SC cells for therapeutic reduction of IOP and treatment of glaucoma.

T. Stack, M. Vincent, Dr. A. Vahabikashi, Prof. M. Johnson, Prof. E. Scott
Department of Biomedical Engineering
Northwestern University
2145 Sheridan Road, Evanston, IL 60208, USA
E-mail: evan.scott@northwestern.edu
Dr. G. Li, K. M. Perkumas, Prof. W. D. Stamer
Department of Ophthalmology
Duke University
2351 Erwin Road, Durham, NC 27710, USA
Prof. W. D. Stamer
Department of Biomedical Engineering
Duke University
101 Science Drive, Durham, NC 27708, USA
Prof. M. Johnson
Department of Ophthalmology
Northwestern University
645 N. Michigan Avenue, Chicago, IL 60611, USA
Prof. M. Johnson
Department of Mechanical Engineering
Northwestern University
2145 Sheridan Road, Evanston, IL 60208, USA
The ORCID identification number(s) for the author(s) of this article can be found under https://doi.org/10.1002/smll.202004205.

DOI: 10.1002/smll.202004205

Glaucoma is the leading cause of irreversible blindness, affecting millions of people worldwide.[1] The elevated intraocular pressure (IOP) characteristic of glaucoma is caused by increased resistance to the outflow of aqueous humor from the eye. This increased resistance is thought to be generated either at or very near the inner wall endothelial lining of SC and has been tied to increased stiffness of the SC endothelial cells and their substrate.[2,3] Mechanistically, it appears that increased stiffness of the SC cells impairs the formation of pores in this endothelial barrier, thereby increasing outflow resistance and IOP.[2]

This pathological defect is not targeted by traditional glaucoma pharmacological therapies that act by either decreasing aqueous humor secretion or by increasing unconventional outflow, a separate pathway by which aqueous humor can flow out of the eye.[4] Rho kinase inhibitors and actin depolymerizers are two classes of drugs recently introduced that relax and soften the outflow tissue cells, thereby lowering aqueous humor outflow resistance.[4,5] While these drugs are effective at lowering the elevated IOP associated with glaucoma, they are hindered by prevalent, local side effects including conjunctival hyperemia, subconjunctival hemorrhages, corneal verticillata and other corneal abnormalities associated with blurry vision including irregularly shaped corneal endothelial cells and guttata-like changes.[6,7]

Due to these adverse off-target effects, we sought to develop and optimize a nanocarrier platform employing a targeting moiety for selective intracellular delivery to SC cells as a glaucoma treatment strategy. Nanomaterials have been shown to be advantageous drug delivery platforms that are well-suited for targeting specific cells and tissues.[8,9] Enhanced targeting and cell specificity allows for less off-target drug delivery and a lower potential for side effects.[10] Targeted nanomaterials have been shown to lower the therapeutic threshold concentration for certain drugs after encapsulation as well as reduce cytotoxicity and other unwanted effects in many cell types including SC cells.[11–13]

Latrunculin is a well-known transient actin depolymerizing agent that mechanically softens cells[14] and has been shown to significantly reduce IOP in animal studies.[5,15] A phase I clinical trial, at concentrations previously found to be effective in primates, found a modest reduction of IOP with side effects

that included mild redness, irritation, and a transient increase in central corneal thickness.[16] We speculated that targeted delivery of latrunculin to SC cells would provide increased bioavailability while minimizing side effects. Self-assembled poly (ethylene glycol)-*b*-poly(propylene sulfide) (PEG-*b*-PPS) block co-polymers have been used as versatile nanocarriers in a wide range of applications.[12,17–23] Depending on the morphology employed, PEG-*b*-PPS nanocarriers can retain both hydrophobic and hydrophilic payloads, respectively, in their cores or aqueous interior compartments[20,21,24–26] and are highly customizable through control of charge, size, and targeting moieties on their surfaces.[8,27] Nanomaterials provide a wide range of options for sustained drug and gene delivery,[19,22,28] and the development of SC targeted nanocarriers will thus provide versatile options for the long term delivery of glaucoma therapeutics following a single intracameral injection. Here, we report on the design and development of a PEG-*b*-PPS controlled delivery system to deliver latrunculin A to SC cells.

SC cells express the lymphatic lineage receptor VEGFR3/FLT4 at moderately high levels as compared with blood vascular cells, which lack this receptor.[29] PEG-*b*-PPS micellar nanocarriers decorated with a FLT4-specific targeting peptide and loaded with latrunculin A were generated. The targeting and functional efficacy of this formulation was assessed in vitro in SC cells using uptake assays and atomic force microscopy (AFM). In vivo efficacy was evaluated using a C57BL/6J mouse model by measuring changes in IOP over multiple days after administering targeted nanocarriers intracamerally. Results show that the targeted nanocarriers were highly selective for SC cells in comparison with blood vascular cells, and that targeted latrunculin-loaded micelles (tLatA-MC) significantly lowered IOP in mouse eyes, as compared to control eyes treated with non-targeted latrunculin-loaded micelles (ntLatA-MC).

Peptide lipid constructs can be attached to PEG-*b*-PPS micelles for intracellular delivery to SC endothelial cells with high efficiency and do not influence micelle structure. VEGFR3/FLT4 is a lymphatic marker that is expressed at the surface of SC endothelial cells.[30,31]We hypothesized that displaying a ligand for this receptor at the micelle surface would enhance micelle uptake selectively by SC cells as compared with other ocular cells, particularly blood vascular cells. We examined the expression of FLT4 in human SC cells and human umbilical vein endothelial cells (HUVEC; used as a generic blood vascular cell control). Schlemm's cells were isolated as previously described[32] and HUVEC were obtained from Lonza (Basel, Switzerland). Cells were prepared as described in the methods (see Supporting Information for all detailed methods) and labeled with anti-FLT4 antibody. FLT4 expression was evaluated using laser scanning confocal microscopy, widefield fluorescence microscopy, and flow cytometry. As expected, FLT4 was present on the SC cell surface at significantly higher abundance than the HUVEC cell surface (**Figure 1**A,B, Figure S1, Supporting Information).

Targeted micelles were developed that incorporated an FLT4-targeting ligand (tBL-MC and tLatA-MC [BL = blank, t = peptide target]; Figure 1C). Several peptide sequences binding FLT4 were previously identified using phage display.[33] The highest affinity peptide sequence, WHWLPNLRHYAS, was selected as a targeting moiety and attached to a palmitoleic acid tail via a PEG spacer (Figure 1D). We have previously used constructs of this format with polymersomes for optimization of cell-selective targeting.[8] This targeting peptide construct was synthesized by solid phase peptide synthesis and was purified using preparatory HPLC. The resulting peptide construct had a mass of 2151 g mol^{-1} as assessed by LC-MS and was of high purity (≥95% pure; Figure 1E). Micelles were formed via the co-solvent evaporation method[34] and separate batches were pooled and then separated into blank MC (BL-MC), non-targeted LatA-MC (nt-LatA-MC), and targeted LatA-MC (tLatA-MC) formulations. tLatA-MC formulations were generated by incubating PEG-*b*-PPS micelles on an end-to-end shaker with 5% molar ratio of the peptide construct to PEG-*b*-PPS copolymer. Latrunculin A content of the micelles was quantified using HPLC as previously described,[11] and loading efficiency was found to vary between 55% and 65% across multiple formulations. Peptide incorporation did not alter latrunculin A content of the micelles (Table S1, Supporting Information).

We next evaluated the tLatA-MC formulations for peptide incorporation using fluorescence spectroscopy. The tryptophan residues on the FLT4 targeting peptide grant the construct an intrinsic fluorescence that can be measured against a standard curve to determine peptide concentrations within the micelles (Figure S2, Supporting Information). Incorporation efficiencies of 91% or above were found for all measured molar ratios (Figure 1F). Formulations were evaluated by transmission electron microscopy (TEM) and dynamic light scattering (DLS) to characterize size, polydispersity, and morphology (Figure 1G). TEM characterization confirmed micelles prepared with peptide form successfully and are not disrupted by peptide embedding (Figure 1G). There were not significant differences in micelle size between the groups (Table S1, Supporting Information). We further characterized the micelle formulations with SAXS using synchrotron radiation (Figure 1H). A core–shell model was fit to each scattering profile, and the core–shell radius and shell thickness of the micelles were estimated. Minimal differences in micelle dimensions were found between blank and peptide-displaying formulations (Figure 1H). These results are consistent with our previous findings that neither Latrunculin A loading nor incorporation of targeting peptide via lipid anchoring alter the size or structure of micelles.[8,11]

tLatA-MC demonstrated significantly greater uptake by SC cells and cell softening compared to non-targeted micelles in vitro. To evaluate the targeting efficacy of the FLT4 binding peptide, we examined the uptake of micelles. SC cells and HUVEC were incubated with 0.5 mg mL^{-1} Alexa 555 labeled micelles incorporated with various molar ratios (1%, 3%, 5%) of peptide to micelle for 1 h at 37 °C. Afterward, cells were washed, harvested, and evaluated for particle uptake and cytotoxicity by flow cytometry. Flow cytometric analysis demonstrated that 5% peptide incorporation into targeted blank micelles (tBL-MC) modestly increased the number of particles internalized by SC cells as compared to ntBL-MC and 1% tBL-MC (**Figure 2**A,B). Peptide incorporation significantly increased the number of particles internalized by SC cells as compared to HUVECs (Figure 2B). This was primarily due to unexpectedly decreased micellar uptake by HUVEC as compared to BL-MCs, which to our knowledge is a phenomenon not previously reported. This result may be related to altered cell membrane interactions caused by the palmitoleic acid in the targeted micelles.[35]

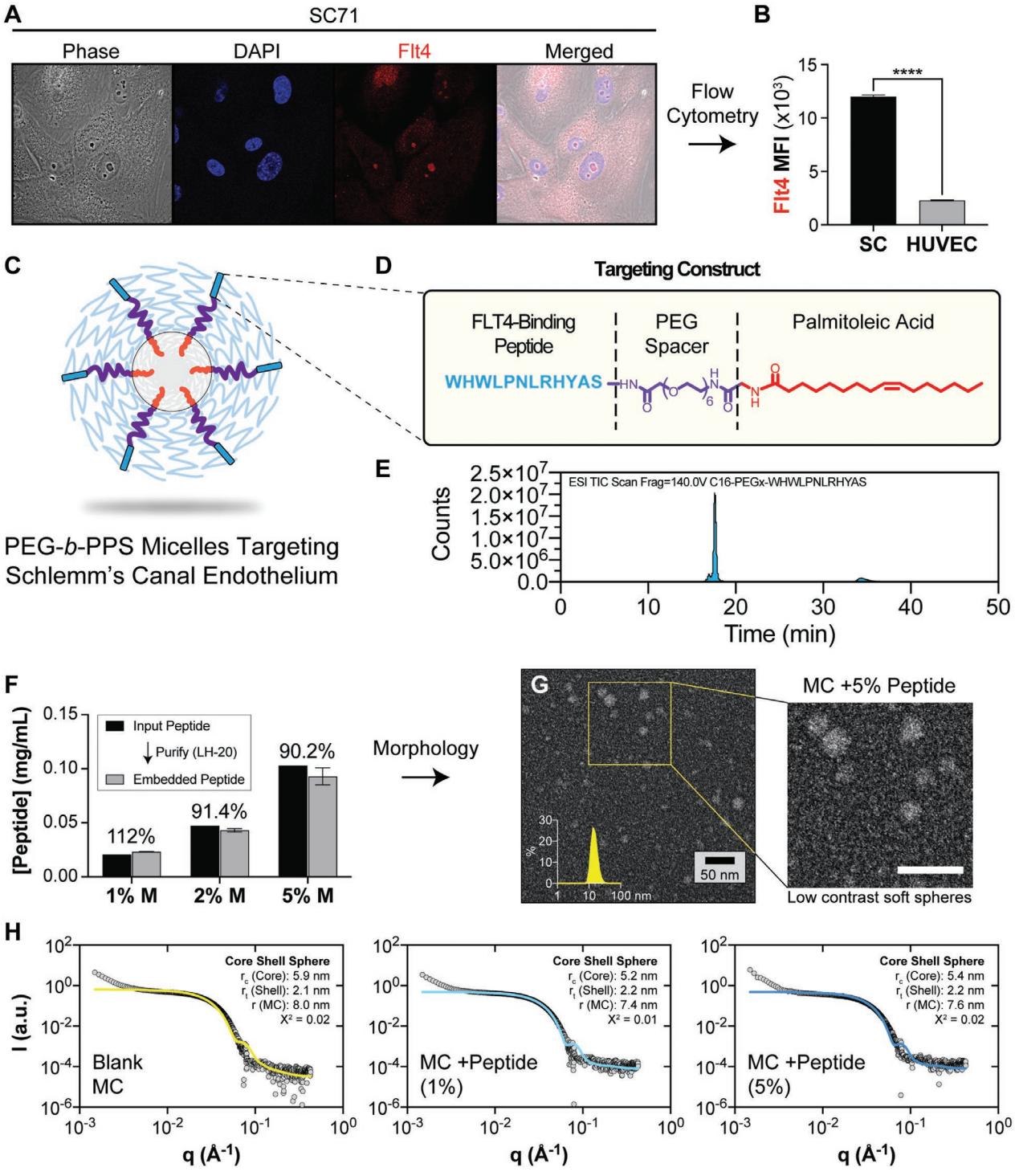

Figure 1. The design of PEG-*b*-PPS micelles that target SC cells in the anterior segment of the eye. A,B) Human SC cells express Flt4/VEGFR3. A) Representative confocal microscopy images of SC endothelial cells that were stained with anti-FLT4 antibody to confirm presence of FLT4 on the cell surface. Cells were stained with Hoescht 33342 (blue) and FLT4 (red). B) Flow cytometry data comparing median fluorescence intensity (MFI) of SC cells and HUVECs stained with anti-FLT4 antibodies. Data shown as mean ± SEM. Significance determined by unpaired *t*-test (****$p < 0.0001$). C) Schematic representation of peptide-displaying micelles. D) The peptide-targeting construct consisting of targeting peptide, PEG spacer, and palmitoleic acid tail. E) LCMS spectra of the purified Flt4-targeting peptide construct. F) Peptide loading efficiency of PEG 6 peptide construct into PEG-*b*-PPS micelles at various molar ratios as determined by tryptophan fluorescence measurements. Data shown as mean ± SD, $N = 3$ technical replicates. G) STEM micrograph of negatively stained PEG-*b*-PPS micelles (MC) displaying the peptide targeting construct (5%; 200 000× magnification). H) Synchrotron small angle x-ray scattering (SAXS) plots for Blank micelles, and micelles displaying the targeting peptide at 1% and 5% molar ratios. A core–shell model (solid line) was fit to the data (gray points). The core radius (r_c), shell thickness (r_t), and total MC radius (r) is displayed together with the chi square (X^2) value for the final model fit.

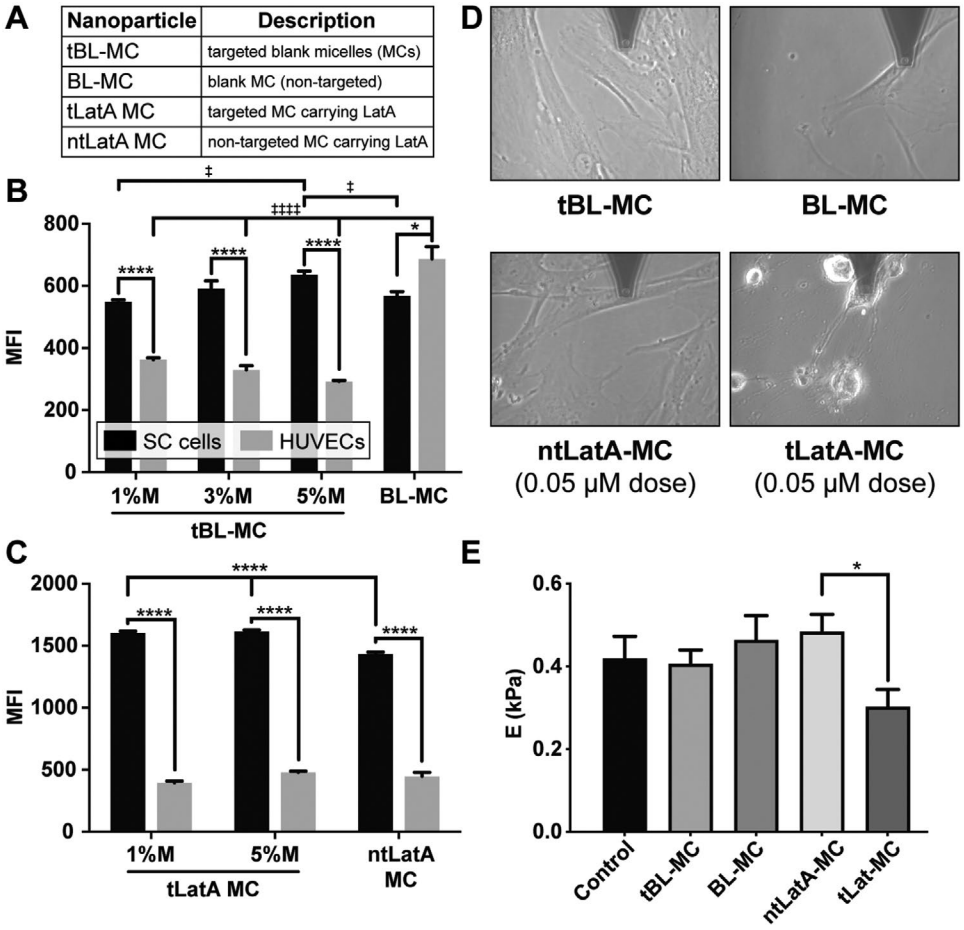

Figure 2. The micellar display of a FLT4-binding peptide targets the delivery of Lat A to SC endothelial cells in vitro. A–C) The FLT4-targeting peptide enhances micelle uptake by SC endothelial cells and decreases uptake by HUVEC. A) Nanoparticle formulation abbreviations. B) unloaded micelles, C) micelles loaded with latrunculin (LatA). Cells were incubated for 1 h with Alexa 555 labeled micelles incorporated with various molar ratios (1%, 3%, 5%) of peptide to micelle. After 1 h incubation, cells were washed, harvested and fixed for analysis via flow cytometry. Median fluorescence intensity (MFI) was measured to quantify uptake of the various formulations by both cell types. Data shown as mean ± SEM ($n = 3$ biological replicates). In (B), significance determined by one-way ANOVA for each of the two cell types with post hoc Tukey's multiple comparisons test (‡‡‡‡$p < 0.0001$, ‡$p < 0.05$). In B, C)Two way ANOVA was used to evaluate differences between all groups with post hoc Sidak's multiple comparisons test (****$p < 0.0001$, *$p < 0.05$). D,E) Targeted delivery of Lat A decreases the stiffness of human SC cells. D) Representative images taken during AFM measurements of cells treated for 2 h with BL-MC, tBL-MC (0.97 mg mL^{-1}), ntLatA-MC, or tLatA-MC (0.05 μM Lat A, 0.97 mg mL^{-1}); AFM tip is at top of each panel. E) Stiffness of SC cells after 2 h was determined by AFM; data shown is geometric mean ± SD (≥ 5 measurements/condition). In (E), significance determined by ANOVA with post hoc Tukey's multiple comparisons test (*$p < 0.05$).

When latrunculin A was loaded into micelles, the uptake by both cell types was altered. The decrease in uptake of targeted micelles (tBL-MC) by HUVECs, as compared with blank micelles (BL-MC), is no longer observed with latrunculin-loaded targeted micelles (tLatA-MC; Figure 2C). In SC cells, there was a statistically significant increase in all cases when peptide was incorporated as compared to blank micelles (Figure 2C). SC cells demonstrated even greater uptake of the Latrunculin A loaded constructs with and without peptide than the HUVEC. This difference increases considerably for the Lat A formulations, suggesting incorporation of Lat A alters the uptake pattern of micelles in both SC cells and HUVECs, perhaps by changing micellar properties that were not examined or through effects of Lat A on the cells. This phenomenon is of significant interest and is currently under additional investigation.

To evaluate the functional effects of tLatA-MC on cultured human SC cells, we used atomic force microscopy (AFM) to assess changes in cell stiffness and morphology.[36] (Figure 2D,E) following treatment of SC cells with tLatA-MC (0.05 μM Latrunculin A and 5% peptide by molar ratio) as compared with concentration-matched ntLatA-MC and micelle controls prepared without Latrunculin A (BL-MC and tBL-MC) or a PBS vehicle control for 2 h. Latrunculin A-induced alterations in cell morphology, particularly the rounding of cell shape, indicative of cell softening,[2,14] was observed by phase contrast microscopy (Figure 2D). At this low concentration of latrunculin, only tLatA-MC significantly reduces SC cell stiffness (Figure 2E). These data show that embedding the targeting peptide into the micelles increases the functional efficacy of the formulation in inducing cell softening of SC cells at low latrunculin concentrations as compared to ntLatA-MC.

We next evaluated the efficacy of our tLatA-MC formulation in vivo. Two different in vivo trials were performed (**Figure 3**A) following animal protocol (A001-19-01) approved by Duke

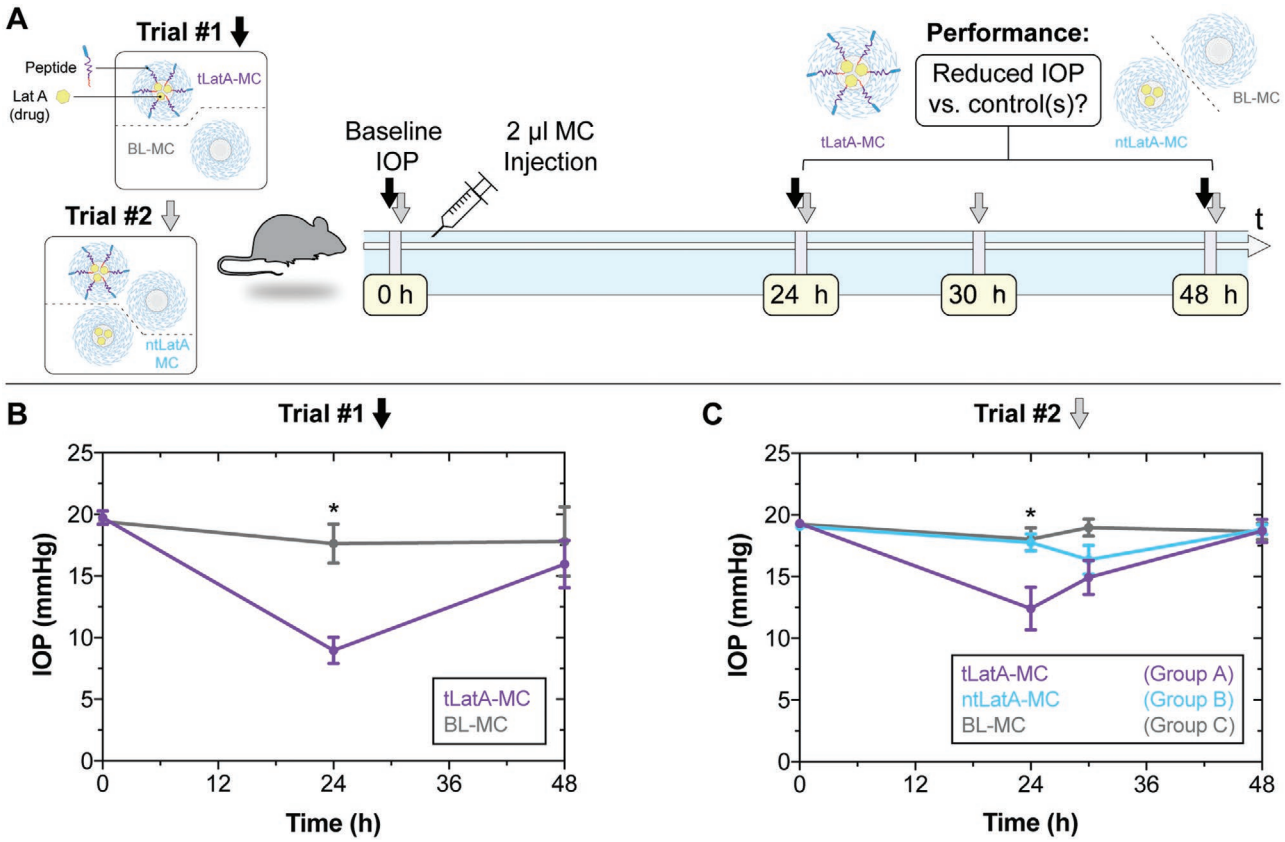

Figure 3. Targeted delivery of latrunculin reduces IOP in mouse eyes. A) Illustrative overview of experiments which consisted of two different IOP measurement schedules. Trials #1 and Trial #2 IOP timepoints shown with black and gray arrows, respectively. B) Trial #1 results. The first trial consisted of 2 µL intracameral injection of BL-MC or tLatA MC (40 mg mL^{-1}, 5% Peptide, 17 µM Lat A) in 5 mice. IOP was measured prior to injection, and after 24 and 48 h. C) Trial #2 results. 2 µL of BL-MC, ntLatA-MC, or tLatA-MC (15.5 µM Lat A, 40 mg mL^{-1} 5% peptide) micelles were injected into 1 eye of 5 mice each. IOP was measured prior to injection and at three timepoints during a 48 h time course. Intraocular pressure (IOP) is measured by rebound tonometry (TonoLab; Icare). Data shown are mean ± SEM ($n = 5$). Trial #1 significance determined by unpaired t-test (*$p < 0.003$). Trial #2 significance determined by ANOVA with post hoc Tukey's multiple comparisons test (*$p < 0.03$).

University. In the first, mice received intracameral injections of targeted latrunculin A-loaded tLatA-MC or blank micelle formulation, ntBL-MC. tLatA-MC significantly decreased IOP by 49% compared to blank MC at 24 h (Figure 3B).

We further evaluated the in vivo efficacy of tLatA-MC in a second trial designed to include non-targeted latrunculin A-loaded micelles, ntLatA-MC (Figure 3A). Trial 2 revealed that tLatA-MC significantly reduced IOP by 30% and 31% compared to ntLatA-MC and BL-MC, respectively, at 24 h (Figure 3C). LatA-MC concentrations for both trials can be found in Figure S3, Supporting Information. Contralateral eyes that did not receive injection showed a consistent baseline for all three groups (Figure S4, Supporting Information). These data indicate that incorporation of FLT4 peptide into latrunculin A-loaded micelle formulations significantly lowered IOP in mice whereas non-targeted micelles did not. These results confirmed our observations in cultured cells probed by AFM (Figure 2D,E), where only peptide-targeted micelles significantly increased the efficacy of encapsulated latrunculin A.

The lack of effect of ntLatA-MC alone was unexpected but could be due to increased uptake in trabecular meshwork cells of ntLatA-MC that leads to a lower than threshold dose of LatA to be delivered to SC cells. Additionally, SC cells are only moderately phagocytic,[11] and the targeting peptide may be required to reach intracellular threshold concentrations necessary for therapeutic effect.

In conclusion, we have successfully developed a targeted PEG-*b*-PPS nanocarrier system loaded with actin depolymerizing/cell softening agent latrunculin A (tLatA-MC). These micellar nanocarriers were designed with an FLT4-binding peptide to target SC cells in the eye. This system can load a variety of hydrophobic drug payloads and targeting moieties. Interestingly, the tBL-MC showed a decrease in HUVEC uptake although tLatA-MC did not. This is to our knowledge a previously unreported phenomenon and suggest that we not only can target the SC cells, but greatly reduce non-specific binding. Further work also must be undertaken to determine if this phenomenon is limited to HUVECs.

The data indicating tLatA-MC reduced IOP in two sets of mouse trials demonstrates the potential clinical significance of this delivery platform. Further studies will be necessary to demonstrate that use of these targeted nanocarriers reduce off target effects, as our data suggest, and also to investigate use of this delivery platform in other settings, particularly those requiring targeted delivery of hydrophobic drugs.

Supporting Information

Supporting Information is available from the Wiley Online Library or from the author.

Acknowledgements

Peptide synthesis and characterization was performed at the Peptide Synthesis Core Facility of the Simpson Querrey Institute at Northwestern University. This facility has current support from the Soft and Hybrid Nanotechnology Experimental (SHyNE) Resource (NSF ECCS-1542205). AFM studies were performed at SPID facility of Northwestern University's NUANCE Center, which has received support from the Soft and Hybrid Nanotechnology Experimental (SHyNE) Resource (NSF ECCS-1542205). This work made use of the IMSERC at Northwestern University, which has received support from the Soft and Hybrid Nanotechnology Experimental (SHyNE) Resource (NSF ECCS-1542205), the State of Illinois, and the International Institute for Nanotechnology (IIN). Funding for in vitro studies was provided by NIH grant 1R01EY019696 while animal studies were funded by 1R0EY022359.

Conflict of Interest

The authors declare no conflict of interest.

Author Contributions

T.S., M.J, and E.S. designed the study. T.S., M.V., M.J., W.D.S., A.V., and E.S. contributed to the writing of the manuscript. T.S., M.V., and A.V. conducted the in vitro experiments. W.D.S. and K.M.P. contributed human SC endothelial cells for use in this study. T.S., M.V., G.L., W.D.S., M.J., and E.S. contributed to the design and execution of the mouse studies.

Keywords

controlled delivery, endothelium, glaucoma, latrunculin, nanoparticle

Received: July 12, 2020
Revised: August 19, 2020
Published online: October 4, 2020

[1] H. A. Quigley, A. T. Broman, *Br. J. Ophthalmol.* **2006**, *90*, 262.
[2] D. R. Overby, E. H. Zhou, R. Vargas-Pinto, R. M. Pedrigi, R. Fuchshofer, S. T. Braakman, R. Gupta, K. M. Perkumas, J. M. Sherwood, A. Vahabikashi, Q. Dang, J. H. Kim, C. R. Ethier, W. D. Stamer, J. J. Fredberg, M. Johnson, *Proc. Natl. Acad. Sci. U. S. A.* **2014**, *111*, 13876.
[3] A. Vahabikashi, A. Gelman, B. Dong, L. Gong, E. D. K. Cha, M. Schimmel, E. R. Tamm, K. Perkumas, W. D. Stamer, C. Sun, H. F. Zhang, H. Gong, M. Johnson, *Proc. Natl. Acad. Sci. U. S. A.* **2019**, *116*, 26555.
[4] A. P. Tanna, M. Johnson, *Ophthalmology* **2018**, *125*, 1741.
[5] J. A. Peterson, B. Tian, A. D. Bershadsky, T. Volberg, R. E. Gangnon, I. Spector, B. Geiger, P. L. Kaufman, *Invest. Ophthalmol. Visual Sci.* **1999**, *40*, 931.
[6] V. Andrés-Guerrero, J. García-Feijoo, A. G. Konstas, *Adv. Ther.* **2017**, *34*, 1049.
[7] A. P. Tanna, H. Esfandiari, K. Teramoto, *J. Glaucoma* **2020**, *29*, e41.
[8] S. Yi, X. Zhang, M. H. Sangji, Y. Liu, S. D. Allen, B. Xiao, S. Bobbala, C. L. Braverman, L. Cai, P. I. Hecker, M. DeBerge, E. B. Thorp, R. E. Temel, S. I. Stupp, E. A. Scott, *Adv. Funct. Mater.* **2019**, *29*, 1904399.
[9] J. Yoo, C. Park, G. Yi, D. Lee, H. Koo, *Cancers* **2019**, *11*, 640.
[10] E. A. Scott, N. B. Karabin, P. Augsornworawat, *Annu. Rev. Biomed. Eng.* **2017**, *19*, 57.
[11] T. Stack, A. Vahabikashi, M. Johnson, E. Scott, *J. Biomed. Mater. Res. A* **2018**, *106*, 1771.
[12] S. D. Allen, Y.-G. Liu, T. Kim, S. Bobbala, S. Yi, X. Zhang, J. Choi, E. A. Scott, *Biomater. Sci.* **2019**, *7*, 657.
[13] S. D. Allen, Y.-G. Liu, S. Bobbala, L. Cai, P. I. Hecker, R. Temel, E. A. Scott, *Nano Res.* **2018**, *11*, 5689.
[14] I. Spector, N. R. Shochet, D. Blasberger, Y. Kashman, *Cell Motil. Cytoskeleton* **1989**, *13*, 127.
[15] J. A. Peterson, B. Tian, J. W. McLaren, W. C. Hubbard, B. Geiger, P. L. Kaufman, *Invest. Ophthalmol. Visual Sci.* **2000**, *41*, 1749.
[16] C. A. Rasmussen, P. L. Kaufman, R. Ritch, R. Haque, R. K. Brazzell, J. L. Vittitow, *Transl. Vis. Sci. Technol.* **2014**, *3*, 1.
[17] E. A. Scott, A. Stano, M. Gillard, A. C. Maio-Liu, M. A. Swartz, J. A. Hubbell, *Biomaterials* **2012**, *33*, 6211.
[18] S. Yi, S. D. Allen, Y.-G. Liu, B. Z. Ouyang, X. Li, P. Augsornworawat, E. B. Thorp, E. A. Scott, *ACS Nano* **2016**, *10*, 11290.
[19] N. B. Karabin, S. Allen, H.-K. Kwon, S. Bobbala, E. Firlar, T. Shokuhfar, K. R. Shull, E. A. Scott, *Nat. Commun.* **2018**, *9*, 624.
[20] A. E. Vasdekis, E. A. Scott, C. P. O'Neil, D. Psaltis, J. A. Hubbell, *ACS Nano* **2012**, *6*, 7850.
[21] S. Allen, M. Vincent, E. Scott, *J. Visualized Exp.* **2018**, https://doi.org/10.3791/57793.
[22] S. Bobbala, S. D. Allen, S. Yi, M. Vincent, M. Frey, N. B. Karabin, E. A. Scott, *Nanoscale* **2020**, *12*, 5332.
[23] S. Yi, N. B. Karabin, J. Zhu, S. Bobbala, H. Lyu, S. Li, Y. Liu, M. Frey, M. Vincent, E. A. Scott, *Front. Bioeng. Biotechnol.* **2020**, *8*, https://doi.org/10.3389/fbioe.2020.00542.
[24] S. Bobbala, S. D. Allen, E. A. Scott, *Nanoscale* **2018**, *10*, 5078.
[25] A. Stano, E. A. Scott, K. Y. Dane, M. A. Swartz, J. A. Hubbell, *Biomaterials* **2013**, *34*, 4339.
[26] D. J. Dowling, E. A. Scott, A. Scheid, I. Bergelson, S. Joshi, C. Pietrasanta, S. Brightman, G. Sanchez-Schmitz, S. D. Van Haren, J. Ninković, D. Kats, C. Guiducci, A. de Titta, D. K. Bonner, S. Hirosue, M. A. Swartz, J. A. Hubbell, O. Levy, *J. Allergy Clin. Immunol.* **2017**, *140*, 1339.
[27] M. P. Vincent, S. Bobbala, N. B. Karabin, M. Frey, Y. Liu, J. O. Navidzadeh, T. Stack, E. A. Scott, *bioRxiv* **2020**, https://doi.org/10.1101/2020.04.24.060772.
[28] A. S. Piotrowski-Daspit, A. C. Kauffman, L. G. Bracaglia, W. M. Saltzman, *Adv. Drug Delivery Rev.* **2020**, https://doi.org/10.1016/j.addr.2020.06.014.
[29] A. Aspelund, T. Tammela, S. Antila, H. Nurmi, V.-M. Leppänen, G. Zarkada, L. Stanczuk, M. Francois, T. Mäkinen, P. Saharinen, I. Immonen, K. Alitalo, *J. Clin. Invest.* **2014**, *124*, 3975.
[30] C. N. Dautriche, Y. Tian, Y. Xie, S. T. Sharfstein, *J. Funct. Biomater.* **2015**, *6*, 963.
[31] K. Kizhatil, M. Ryan, J. K. Marchant, S. Henrich, S. W. M. John, *PLoS Biol.* **2014**, *12*, e1001912.
[32] W. D. Stamer, B. C. Roberts, D. N. Howell, D. L. Epstein, *Invest. Ophthalmol. Visual Sci.* **1998**, *39*, 1804.
[33] L.-F. Shi, Y. Wu, C.-Y. Li, *J. Gynecol. Oncol.* **2015**, *26*, 327.
[34] S. Cerritelli, D. Velluto, J. A. Hubbell, *Biomacromolecules* **2007**, *8*, 1966.
[35] G. Sahay, E. V. Batrakova, A. V. Kabanov, *Bioconjugate Chem.* **2008**, *19*, 2023.
[36] R. Vargas-Pinto, H. Gong, A. Vahabikashi, M. Johnson, *Biophys. J.* **2013**, *105*, 300.

